Proc. Camb. Phil. Soc. (1969), **66**, 493
PCPS 66–59
With 3 text-figures
Printed in Great Britain

The space group corepresentations of antiferromagnetic NiO

BY A. P. CRACKNELL AND S. J. JOSHUA
Department of Physics, University of Essex, Wivenhoe Park, Colchester, Essex

(*Received* 10 *July* 1968)

Abstract. The geometry of the Brillouin zone of antiferromagnetic NiO (C_c2/c) is studied. The corepresentations of the magnetic little group are deduced for the points and lines of symmetry. The magnon symmetries are investigated and the selection rules for two magnon electric dipole and magnetic dipole absorption are deduced.

1. *Introduction.* The transition element oxides MnO, FeO, CoO and NiO are known to be antiferromagnetic substances (**11**) and their spin arrangements have been studied by neutron diffraction experiments (**13, 15**). Previous work on these oxides has chiefly been centred on neutron diffraction and susceptibility experiments and the crystal deformation which takes place on magnetic ordering (**11–13, 15**). In the present work particular emphasis is laid on the symmetry properties of NiO both above and below the Néel temperature T_N. Our aim is to study the magnon degeneracies from a knowledge of the symmetry of antiferromagnetic NiO.

2. *Magnetic properties of* NiO. NiO is an antiferromagnet with a Néel temperature, $T_N = 523\,°\text{K}$. Above T_N NiO has the NaCl structure ($Fm3m$, O_h^5) whereas below T_N the crystal becomes slightly distorted from the cubic structure to a rhombohedral one (**12**). This deformation is presumably due to magnetostriction which accompanies the magnetic ordering, and the amount of the distortion is found to increase with decreasing temperature. The distortion consists of contraction of the original cubic unit cell along any one of the four $\langle 111 \rangle$ axes.

The antiferromagnetic ordering of the magnetic moments in NiO is shown in Fig. 1. Only the magnetic ions are shown. The spins of all the ions represented by solid circles are parallel to one another and antiparallel to the spins of all the ions represented by open circles. This antiferromagnetic structure is compatible with the neutron diffraction experiments of Roth (**13**). The spins in NiO are arranged in ferromagnetic sheets parallel to the (111) plane (**13, 15, 18–20**). Roth (**13**) showed from his neutron diffraction data that the direction of sublattice magnetization of each of the ferromagnetic (111) sheets was actually in the plane of the ferromagnetic sheet and he assumed that it was parallel or antiparallel to $[1\bar{1}0]$. Later, from the observed behaviour of S-domains in applied magnetic fields, Yamada (**19**) and Yamada, Saito and Shimomura (**20**) showed that the direction of sublattice magnetization was parallel or antiparallel to $[11\bar{2}]$ and not to $[1\bar{1}0]$. This means that within each ferromagnetic (111) sheet the spins are aligned

https://doi.org/10.1017/S0305004100045229 Published online by Cambridge University Press

in the direction of the intersection of the sheet with the vertical plane through the z-axis and [110]. We shall then classify the eigenstates of the crystal both above and below T_N by finding the irreducible corepresentations of the group of the wave vector for each of the points and lines of symmetry of the Brillouin zone of the appropriate magnetic space group of NiO (7).

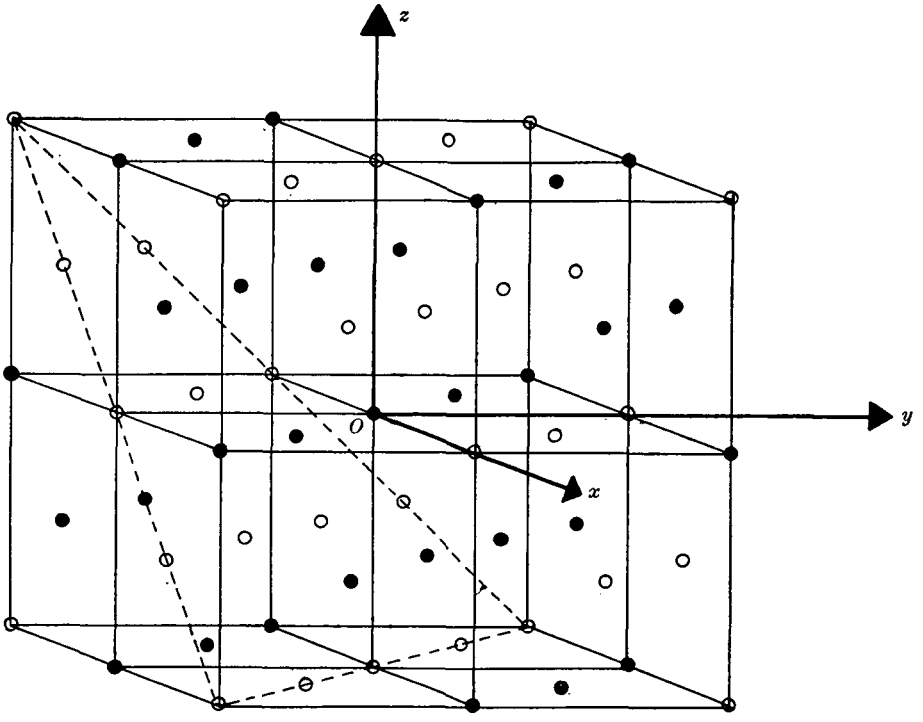


Fig. 1. The two sublattices of antiferromagnetic NiO. Ni^{2+} ions on one sublattice are represented by solid dots and Ni^{2+} ions on the other sublattice by open circles; O^{2-} ions are omitted.

3. *Irreducible corepresentations of the magnetic space groups of* NiO. (i) *Above* T_N. The iron group oxides MnO, FeO, CoO and NiO have the NaCl structure above the Néel temperature. The non-magnetic unit cell therefore has the face-centred cubic Bravais lattice. In terms of unit vectors **i**, **j** and **k** along the x-, y- and z-axes the primitive translations can be defined as

$$\left.\begin{aligned} \mathbf{t}_1 &= \tfrac{1}{2}a(\mathbf{i}+\mathbf{j}), \\ \mathbf{t}_2 &= \tfrac{1}{2}a(-\mathbf{j}+\mathbf{k}), \\ \mathbf{t}_3 &= \tfrac{1}{2}a(-\mathbf{i}+\mathbf{k}), \end{aligned}\right\} \tag{1}$$

where a is the length of a cube edge. As the Brillouin zone for the face-centred cubic Bravais lattice is given in several places (3, 9, 17) we shall not reproduce it here. We summarize in Table 1 the important points and lines of symmetry in the Brillouin zone of the face-centred cubic Bravais lattice (1, 3, 9). The space group of this lattice

https://doi.org/10.1017/S0305004100045229 Published online by Cambridge University Press

is $Fm3m(O_h^5)$. This being a symmorphic space group we need consider only the product of the point-group operations of $m3m$ with $\{E|\mathbf{T}_{n_1 n_2 n_3}\}$ of the translation group where

$$\mathbf{T}_{n_1 n_2 n_3} = n_1\mathbf{t}_1 + n_2\mathbf{t}_2 + n_3\mathbf{t}_3 \tag{2}$$

where n_1, n_2 and n_3 are integers.

Table 1. *Points and lines of symmetry in the Brillouin zone of F.C.C.* NiO (*above* T_N)

Point or line of symmetry	**k**	Group of **k**
Γ	$(2\pi/a)(0,0,0)$	$m3m(O_h)$
Λ	$(2\pi/a)(\alpha,\alpha,\alpha)$	$3m(C_{3v})$
L	$(2\pi/a)(\frac{1}{2},\frac{1}{2},\frac{1}{2})$	$\bar{3}m(D_{3d})$
Δ	$(2\pi/a)(0,\beta,0)$	$4mm(C_{4v})$
X	$(2\pi/a)(0,1,0)$	$4/mmm(D_{4h})$
Σ	$(2\pi/a)(\alpha,\alpha,0)$	$2mm(C_{2v})$
K	$(2\pi/a)(\frac{3}{4},\frac{3}{4},0)$	$2mm(C_{2v})$
W	$(2\pi/a)(\frac{1}{2},1,0)$	$\bar{4}2m(D_{2d})$
Z	$(2\pi/a)(\alpha,1,0)$	$2mm(C_{2v})$
S	$(2\pi/a)(\alpha,1,\alpha)$	$2mm(C_{2v})$
U	$(2\pi/a)(\frac{1}{2},1,\frac{1}{2})$	$2mm(C_{2v})$
Q	$(2\pi/a)(\frac{1}{2},\frac{1}{2}+\alpha,\frac{1}{2}-\alpha)$	$2(C_2)$

The paramagnetic space group has in addition to the above operations their products with the time-reversal operator θ; this is just the grey space group $Fm3'm$ in the notation of Shubnikov and Belov (**14**). The little co-group, $\bar{\mathbf{G}}^{\mathbf{k}}$, for any point or line of symmetry in $Fm3m$ is one of the 32 point groups. Therefore the magnetic little co-group, $\bar{\mathbf{M}}^{\mathbf{k}}$, for any point or line of symmetry in $Fm3'm$ is simply related to the little co-group, $\bar{\mathbf{G}}^{\mathbf{k}}$, for that point or line in $Fm3m$. There are two possibilities. If **k** is a point of symmetry for which **k** is equivalent to $-\mathbf{k}$, i.e. **k** and $-\mathbf{k}$ are separated by a reciprocal lattice vector, then $\bar{\mathbf{M}}^{\mathbf{k}}$ in $Fm3'm$ is simply the grey point group derived from $\bar{\mathbf{G}}^{\mathbf{k}}$ for that point of symmetry in $Fm3m$. If **k** is a point or line of symmetry for which **k** is not equivalent to $-\mathbf{k}$ then $\bar{\mathbf{M}}^{\mathbf{k}}$ is one of the 58 black and white groups and can be written as

$$\bar{\mathbf{M}}^{\mathbf{k}} = \bar{\mathbf{G}}^{\mathbf{k}} + \theta I\bar{\mathbf{G}}^{\mathbf{k}}, \tag{3}$$

where $\bar{\mathbf{G}}^{\mathbf{k}}$ is the little co-group for that point or line of symmetry in $Fm3m$ and I is the inversion operation. In either case the irreducible corepresentations of $\bar{\mathbf{M}}^{\mathbf{k}}$ can then easily be written down since the irreducible corepresentations of the grey point groups and of the black and white point groups have been given by various authors (**5, 6, 8**).

(ii) *Below* T_N. The antiferromagnetic structure of NiO below T_N is shown in Fig. 1; this structure has two magnetic sublattices and the magnetic unit cell is twice as large as the chemical unit cell. As mentioned earlier, below T_N the crystal becomes slightly distorted from the cubic structure to a rhombohedral one, the distortion being temperature sensitive. At room temperature the rhombohedral angle α is about 90° 4·2′ and the unit cell is a slightly distorted cube. The variation of the lattice

https://doi.org/10.1017/S0305004100045229 Published online by Cambridge University Press

constant a and the rhombohedral angle α with temperature has been given by Slack (16). His results are summarized in Table 2 for three different temperatures. To preserve the trigonal symmetry the directions of sublattice magnetization would have

Table 2. *Values of lattice constant a and rhombohedral angle α at three different temperatures [after Slack (16)]*

Temp. (°K)	a (Å)	α
0	4·1725	90° 6′
297	4·177	90° 4·2′
523	4·193	90°

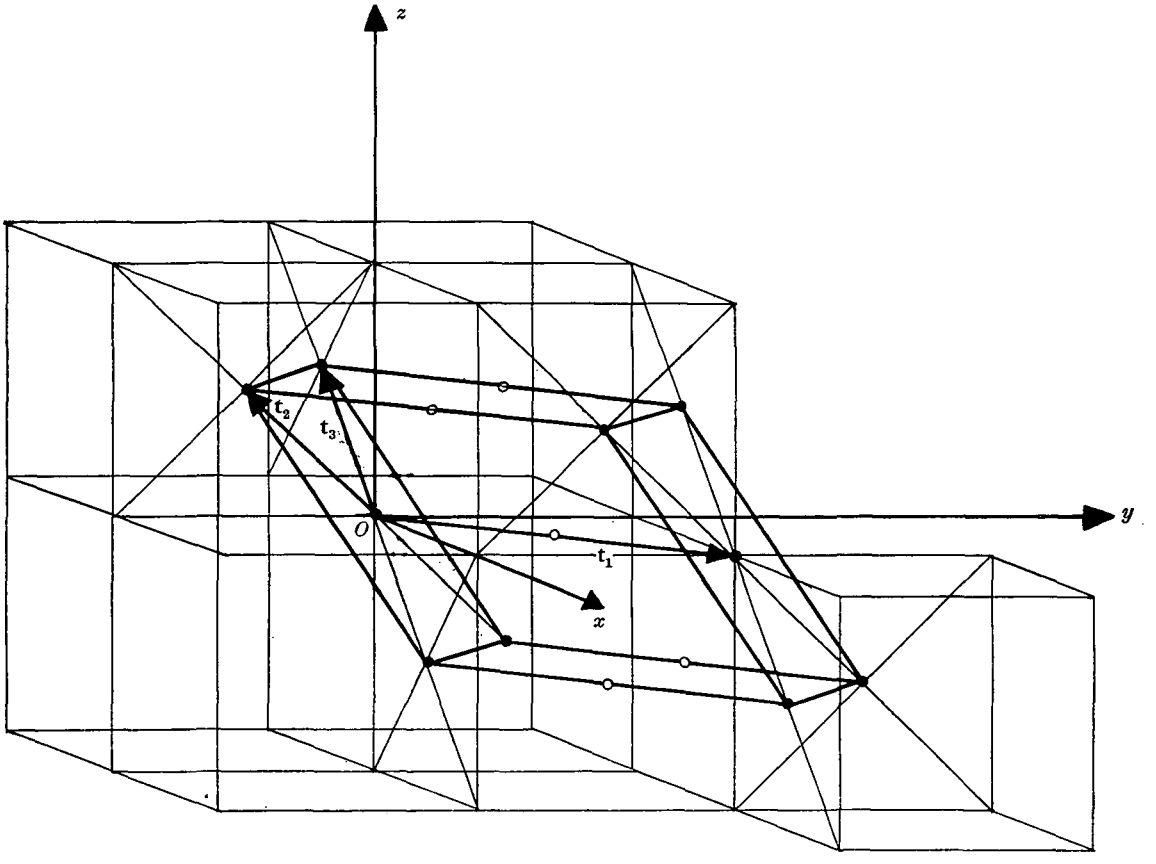


Fig. 2. The unit cell of the magnetic space group of antiferromagnetic NiO.

to be along [111]. However, since the direction of sublattice magnetization is $[11\bar{2}]$ (19, 20) the symmetry group of the ordered phase is $C_c 2/c$ and, in principle at least, further distortions of the lattice could occur, although such distortions appear to be too small to be observed experimentally.

https://doi.org/10.1017/S0305004100045229 Published online by Cambridge University Press

The unit cell corresponding to the black and white magnetic space group $C_c 2/c$ is shown in Fig. 2. The primitive translations are defined as

$$\left.\begin{aligned} \mathbf{t}_1 &= a(\mathbf{i}+\mathbf{j}), \\ \mathbf{t}_2 &= \tfrac{1}{2}a(-\mathbf{j}+\mathbf{k}), \\ \mathbf{t}_3 &= \tfrac{1}{2}a(-\mathbf{i}+\mathbf{k}), \end{aligned}\right\} \tag{4}$$

where we neglect the very small distortions.

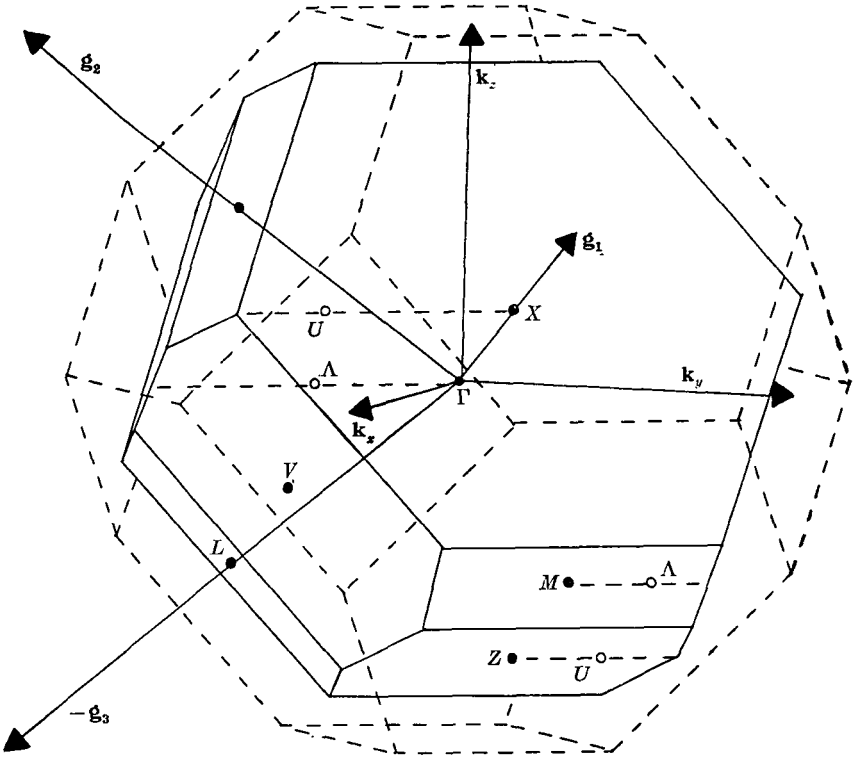


Fig. 3. The Brillouin zone of antiferromagnetic NiO; the paramagnetic Brillouin zone is indicated in broken lines.

The Brillouin zone corresponding to this magnetic structure is shown in Fig. 3. The reciprocal lattice vectors are

$$\left.\begin{aligned} \mathbf{g}_1 &= (2\pi/a)(\tfrac{1}{2}\mathbf{i}+\tfrac{1}{2}\mathbf{j}+\tfrac{1}{2}\mathbf{k}), \\ \mathbf{g}_2 &= (2\pi/a)(\mathbf{i}-\mathbf{j}+\mathbf{k}), \\ \mathbf{g}_3 &= (2\pi/a)(-\mathbf{i}+\mathbf{j}+\mathbf{k}). \end{aligned}\right\} \tag{5}$$

Since we have ignored the small distortions from the cubic dimensions the geometrical shape of the magnetic Brillouin zone in Fig. 3 does have a three-fold axis along $\mathbf{g}_1$ and, indeed if the direction of sublattice magnetization were along the [111] direction then the crystal would be described by a trigonal (rhombohedral) magnetic space group. However, the spins have been assumed to be in some direction in the vertical plane

https://doi.org/10.1017/S0305004100045229 Published online by Cambridge University Press

through $\mathbf{g}_1$ so that the existence of a three-fold axis along $\mathbf{g}_1$ is incompatible with the symmetry of the spin system. In the notation of Dimmock and Wheeler (7) the magnetic structure has the following point-group symmetry operations, E, C_{2b}, I, σ_{db}, which make up the point group $2/m(C_{2h})$. The magnetic space group of this structure

Table 3. *Symmetry points in the magnetic Brillouin zone of* NiO (*below* T_N)

Point or line of symmetry	k	k	$\bar{\mathbf{G}}^{\mathbf{k}}$
Γ	$(2\pi/a)(0,0,0)$	0	$E, C_{2b}, I, \sigma_{db}$
M	$(2\pi/a)(\frac{1}{2},\frac{1}{2},-\frac{1}{2})$	$\mathbf{g}_1-\frac{1}{2}\mathbf{g}_2-\frac{1}{2}\mathbf{g}_3$	$E, C_{2b}, I, \sigma_{db}$
X	$(2\pi/a)(\frac{1}{4},\frac{1}{4},\frac{1}{4})$	$\frac{1}{2}\mathbf{g}_1$	$E, C_{2b}, I, \sigma_{db}$
Z	$(2\pi/a)(\frac{1}{4},\frac{1}{4},-\frac{3}{4})$	$\frac{1}{2}\mathbf{g}_1-\frac{1}{2}\mathbf{g}_2-\frac{1}{2}\mathbf{g}_3$	$E, C_{2b}, I, \sigma_{db}$
L	$(2\pi/a)(\frac{1}{2},-\frac{1}{2},-\frac{1}{2})$	$-\frac{1}{2}\mathbf{g}_3$	E, I
V	$(2\pi/a)(\frac{3}{4},-\frac{1}{4},-\frac{1}{4})$	$\frac{1}{2}\mathbf{g}_1-\frac{1}{2}\mathbf{g}_3$	E, I
Λ	$(2\pi/a)(\alpha,-\alpha,0)$	$\alpha(\mathbf{g}_2-\mathbf{g}_3)$	E, C_{2b}
U	$(2\pi/a)(\alpha,-\alpha,\frac{1}{4})$	$\frac{1}{2}\mathbf{g}_1+\alpha(\mathbf{g}_2-\mathbf{g}_3)$	E, C_{2b}
B	$(2\pi/a)(\frac{1}{2}\alpha,\frac{1}{2}\alpha,\frac{1}{2}\alpha+2\beta)$	$\alpha\mathbf{g}_1+\beta(\mathbf{g}_2+\mathbf{g}_3)$	E, σ_{db}

Table 4. *Character table for* Γ *and* M

Γ	Γ_1^+	Γ_2^+	Γ_1^-	Γ_2^-	Γ_3^+	Γ_4^+	Γ_3^-	Γ_4^-
$\{E\|0\}$	1	1	1	1	1	1	1	1
$\{\bar{E}\|0\}$	1	1	1	1	−1	−1	−1	−1
$\{C_{2b}\|\tau\}$	1	−1	1	−1	i	$-i$	i	$-i$
$\{\bar{C}_{2b}\|\tau\}$	1	−1	1	−1	$-i$	i	$-i$	i
$\{I\|0\}$	1	1	−1	−1	1	1	−1	−1
$\{\bar{I}\|0\}$	1	1	−1	−1	−1	−1	1	1
$\{\sigma_{db}\|\tau\}$	1	−1	−1	1	i	$-i$	$-i$	i
$\{\bar{\sigma}_{db}\|\tau\}$	1	−1	−1	1	$-i$	i	i	$-i$
Coreps	a	a	a	a	c	$-c$	c	$-c$

$M(\mathbf{g}_1-\frac{1}{2}\mathbf{g}_2-\frac{1}{2}\mathbf{g}_3)$
Direct product of $(\{E|0\}+\{E|\mathbf{t}_n\})$ with the group $\bar{\mathbf{M}}^{\mathbf{k}}$ for Γ ($n = 2$ or 3).
Coreps: same as Γ.

is based on the black and white monoclinic Bravais lattice C_c (14) and is $C_c 2/c$ which contains the elements

$$\left.\begin{aligned}\mathbf{M} = \{E|0\},\quad \{C_{2b}|\boldsymbol{\tau}\},\quad \{I|0\},\quad \{\sigma_{db}|\boldsymbol{\tau}\},\\ \theta\{E|\boldsymbol{\tau}\},\quad \theta(C_{2b}|0\},\quad \theta\{I|\boldsymbol{\tau}\},\quad \theta\{\sigma_{db}|0\},\end{aligned}\right\} \tag{6}$$

together with the products of these elements with $\{E|\mathbf{T}_{n_1 n_2 n_3}\}$ and $\{\bar{E}|\mathbf{T}_{n_1 n_2 n_3}\}$. In equation (6) $\boldsymbol{\tau} = \frac{1}{2}a(\mathbf{i}+\mathbf{j}) = \frac{1}{2}\mathbf{t}_1$ and is a non-primitive translation which carries a black (white) Bravais lattice point to a position formerly occupied by a white (black) Bravais lattice point and $\mathbf{t}_1$, $\mathbf{t}_2$ and $\mathbf{t}_3$ are the primitive translation vectors of the antiferromagnetic structure shown in Fig. 2. In Table 3 the coordinates of the special points and lines of symmetry are given and the elements of $\bar{\mathbf{G}}^{\mathbf{k}}$ are identified; these are the unitary elements of $\bar{\mathbf{M}}^{\mathbf{k}}$ and the anti-unitary elements of $\bar{\mathbf{M}}^{\mathbf{k}}$ are given by

https://doi.org/10.1017/S0305004100045229 Published online by Cambridge University Press

multiplying $\overline{\mathbf{G}}^{\mathbf{k}}$ by $\theta\{I|\boldsymbol{\tau}\}$. In Tables 4–7 we give the character table of the unitary subgroup $\overline{\mathbf{G}}^{\mathbf{k}}$ of the wave vector for each of the points and lines of symmetry for the magnetic space group C_c2/c shown in Fig. 3. $\overline{\mathbf{M}}^{\mathbf{k}}$ can be identified for each of the points of symmetry from Table 3 and the last row of each of Tables 4–7 indicates whether the irreducible corepresentations of $\overline{\mathbf{M}}^{\mathbf{k}}$ belong to case (*a*), case (*b*) or case (*c*) (5–8).

Table 5. *Character table for X and Z*

Z ($n = 1, 2$ or 3) ...	Z_1	Z_2
X ($n = 1$)	X_1	X_2
$\{E\|0\}$	2	2
$\{\bar{E}\|0\}$	2	−2
$\{E\|\mathbf{t}_n\}$	−2	−2
$\{\bar{E}\|\mathbf{t}_n\}$	−2	2
$\{C_{2b}\|\boldsymbol{\tau}\}$, $\{C_{2b}\|\boldsymbol{\tau}+\mathbf{t}_n\}$	0	0
$\{\bar{C}_{2b}\|\boldsymbol{\tau}\}$, $\{\bar{C}_{2b}\|\boldsymbol{\tau}+\mathbf{t}_n\}$	0	0
$\{I\|0\}$	0	0
$\{\bar{I}\|0\}$	0	0
$\{I\|\mathbf{t}_n\}$	0	0
$\{\bar{I}\|\mathbf{t}_n\}$	0	0
$\{\sigma_{db}\|\boldsymbol{\tau}\}$, $\{\sigma_{db}\|\boldsymbol{\tau}+\mathbf{t}_n\}$	0	0
$\{\bar{\sigma}_{db}\|\boldsymbol{\tau}\}$, $\{\bar{\sigma}_{db}\|\boldsymbol{\tau}+\mathbf{t}_n\}$	0	0
Coreps X	*a*	*a*
Coreps Z	*a*	*a*

Table 6. *Character table for L and V*

L ($n = 3$)	L_1^+	L_1^-	L_2^+	L_2^-
V ($n = 1$ or 3)	V_1^+	V_1^-	V_2^+	V_2^-
$\{E\|0\}$	1	1	1	1
$\{\bar{E}\|0\}$	1	1	−1	−1
$\{E\|\mathbf{t}_n\}$	−1	−1	−1	−1
$\{\bar{E}\|\mathbf{t}_n\}$	−1	−1	1	1
$\{I\|0\}$	1	−1	1	−1
$\{\bar{I}\|0\}$	1	−1	−1	1
$\{I\|\mathbf{t}_n\}$	−1	1	−1	1
$\{\bar{I}\|\mathbf{t}_n\}$	−1	1	1	−1
Coreps L	*a*	*a*	*a*	*a*
Coreps V	*c*	*c*	*c*	*c*

We now study in a little more detail the symmetry of the magnetic Brillouin zone of NiO illustrated in Fig. 3. In this figure we show the antiferromagnetic Brillouin zone inside the paramagnetic face-centred cubic Brillouin zone; $\mathbf{g}_2$ and $\mathbf{g}_3$ of equation (5) are the same as would be obtained for the cubic paramagnetic phase, while $\mathbf{g}_1$ is half of the corresponding $\mathbf{g}_1$ for the cubic phase. The volume of the antiferromagnetic Brillouin zone is thus half of the volume of the Brillouin zone of the cubic phase. Therefore, in general, the zone boundaries will be closer to Γ than in the para-

https://doi.org/10.1017/S0305004100045229 Published online by Cambridge University Press

magnetic phase. In terms of the reduced wave vector ζ the phonon Brillouin zone boundaries in the [001], [110] and [111] directions for

$$\mathbf{k} = (2\pi/a)(0, 0, \zeta), \quad \mathbf{k} = (2\pi/a)(\zeta, \zeta, 0) \quad \text{and} \quad \mathbf{k} = (2\pi/a)(\zeta, \zeta, \zeta)$$

occur at $\zeta = 1{\cdot}0$, $\zeta = 0{\cdot}75$ and $\zeta = 0{\cdot}5$ respectively. For the magnetic Brillouin zone shown in Fig. 3 the boundaries are at $\zeta = 0{\cdot}75$ in the [001] direction, at $\zeta = 0{\cdot}375$ in the [110] direction, and $\zeta = 0{\cdot}25$ in the [111] direction. Because [111] is along the

Table 7. *Character tables for* Λ, U *and* B

Λ ...	Λ_1	Λ_2	Δ_3	Λ_4
$\{E\|0\}$	1	1	1	1
$\{\bar{E}\|0\}$	1	1	-1	-1
$\{C_{2b}\|\tau\}$	1	-1	i	$-i$
$\{\bar{C}_{2b}\|\tau\}$	1	-1	$-i$	i
Coreps Λ	a	a	c	$-c$
U ...	U_1	U_2	U_3	U_4
$\{E\|0\}$	1	1	1	1
$\{\bar{E}\|0\}$	1	1	-1	-1
$\{C_{2b}\|-\tau\}$	i	$-i$	-1	1
$\{\bar{C}_{2b}\|-\tau\}$	i	$-i$	1	-1
Coreps U	a	a	c	$-c$
B ...	B_1	B_2	B_3	B_4
$\{E\|0\}$	1	1	1	1
$\{\bar{E}\|0\}$	1	1	-1	-1
$\{\sigma_{db}\|\tau\}$	ξ	$-\xi$	$i\xi$	$-i\xi$
$\{\bar{\sigma}_{db}\|\tau\}$	ξ	$-\xi$	$-i\xi$	$i\xi$
Coreps B	a	a	c	$-c$

$\xi = \exp(-i\mathbf{k}.\tau)$.

direction of $\mathbf{g}_1$ the magnon dispersion curves along [111] from $\zeta = 0$ to $\zeta = 0{\cdot}5$ should be symmetrical about $\zeta = 0{\cdot}25$ and therefore flat at $\zeta = 0{\cdot}25$. The behaviour of the magnon branches along [001] for $\zeta > 0{\cdot}75$ and along [110] for $\zeta > 0{\cdot}375$ is more complicated because these are not along the direction of a reciprocal lattice vector and there is no reflexion plane of symmetry normal to either of these directions. The magnon branches in these directions are therefore not symmetrical about $\zeta = 0{\cdot}75$ for the [001] direction nor about $\zeta = 0{\cdot}375$ for the [110] direction neither are the branches flat at these points. The magnon branches as calculated directly by Begum and Reissland (2) do exhibit just the symmetry properties that we have described above for the [111], [110] and [001] directions. The six directions which were [110], [011], [101], [$1\bar{1}0$], [$10\bar{1}$] and [$0\bar{1}1$] in the cubic phase and which cut the Brillouin zone boundaries at a distance of $\frac{3}{4}\sqrt{2}(2\pi/a)$ from Γ in the cubic phase are now different and cut the Brillouin zone boundaries at different distances from Γ. If we ignore the distortions then [110], [011] and [101] cut the Brillouin zone boundary at $\frac{3}{8}\sqrt{2}(2\pi/a)$ from Γ, while [$1\bar{1}0$],

https://doi.org/10.1017/S0305004100045229 Published online by Cambridge University Press

$[10\bar{1}]$ and $[0\bar{1}1]$ cut the Brillouin zone boundary at $\frac{11}{16}\sqrt{2}\,(2\pi/a)$ from Γ. There will thus be different dispersion curves for the magnon frequency ν against $\mathbf{k}$ in these directions. A multi-domain structure can exist below the Néel temperature even in a crystal which is, crystallographically speaking, a single crystal because as the crystal is cooled below its Néel temperature there is a choice of four equivalent directions, [111], $[\bar{1}11]$, $[1\bar{1}1]$ and $[11\bar{1}]$, for the normal to the ferromagnetic sheets. In different parts of the crystal a different one of these directions might be chosen so that one obtains a crystal that magnetically has a domain structure while being crystallographically a single crystal.

4. *The symmetries of magnons in antiferromagnetic* NiO. We seek to determine the symmetries of the magnons in NiO and this can be done by assigning the magnon creation operators (10)

$$\alpha^{\dagger}_{\downarrow\mathbf{k}} = \frac{1}{\sqrt{(2SN)}}\{u_{\mathbf{k}}\sum_i \exp(i\mathbf{k}\,.\,\mathbf{r}_i)\,S_i^- - v_{\mathbf{k}}\sum_j \exp(i\mathbf{k}\,.\,\mathbf{r}_j)S_j^-\} \tag{7}$$

and

$$\alpha^{\dagger}_{\uparrow\mathbf{k}} = \frac{1}{\sqrt{(2SN)}}\{u_{\mathbf{k}}\sum_j \exp(i\mathbf{k}\,.\,\mathbf{r}_j)S_j^+ - v_{\mathbf{k}}\sum_i \exp(i\mathbf{k}\,.\,\mathbf{r}_i)S_i^+\} \tag{8}$$

to the irreducible corepresentations of $\bar{\mathbf{M}}^{\mathbf{k}}$, where i and j refer to the two sublattices. S^+ and S^- are given by

$$\left.\begin{aligned} S^+ &= S_\xi + iS_\eta, \\ S^- &= S_\xi - iS_\eta, \end{aligned}\right\} \tag{9}$$

where ξ, ζ and η form a right-handed orthogonal set of axes and ξ is along the direction of sublattice magnetization. We choose η along the two-fold rotation axis C_{2b} and this fixes the direction of ζ. The effect of the rotational parts of space-group operations in equation (6) on S^+ and S^- can readily be seen to be

$$\left.\begin{aligned} ES^+ &= S^+, & ES^- &= S^-, \\ C_{2b}S^+ &= -S^-, & C_{2b}S^- &= -S^+, \\ IS^+ &= S^+, & IS^- &= S^-, \\ \sigma_{db}S^+ &= -S^-, & \sigma_{db}S^- &= -S^+. \end{aligned}\right\} \tag{10}$$

Therefore by studying the transformation properties of $\alpha^{\dagger}_{\downarrow\mathbf{k}}$ and $\alpha^{\dagger}_{\uparrow\mathbf{k}}$ under the members of $\bar{\mathbf{M}}^{\mathbf{k}}$ the magnons in NiO can be assigned to the correct irreducible corepresentations of $\bar{\mathbf{M}}^{\mathbf{k}}$ and the results are given in Table 8.

5. *Selection rules for two-magnon absorption.* Of particular interest to experimentalists are the selection rules for the creation of two magnons with equal and opposite $\mathbf{k}$ vectors by the absorption of a photon. The selection rule for two-magnon electric dipole absorption for a general wave vector $\mathbf{k}$ has been discussed by Loudon (10). The momentum of the incoming photon is so small that the two magnons that are created have equal and opposite $\mathbf{k}$ vectors. For each of the special points of symmetry in the magnetic Brillouin zone $\mathbf{k}$ and $-\mathbf{k}$ are equivalent so that, to all intents and purposes, the two magnons are created at the same special point. The components of the electric dipole operator transform like ξ, η and ζ, i.e. like Γ_2^-, Γ_1^- and

https://doi.org/10.1017/S0305004100045229 Published online by Cambridge University Press

Γ_2^- respectively, while the components of the magnetic dipole operator transform like L_ξ, L_η and L_ζ, i.e. like Γ_2^+, Γ_1^+ and Γ_2^+ respectively. For each of the points M, X, Z, L and V we give in Table 9 the ordinary Kronecker product $R_i \otimes R_j$ for each of the representations given in Table 8. We also give the symmetrized square $[R_i]^2$ for the degenerate representations and note that for non-degenerate representations, i.e. at M, L and V

$$[R_i]^2 = R_i \otimes R_i. \tag{11}$$

Table 8. *Magnon symmetries in* NiO

Point or line	Magnon
Γ	Γ_1^+, Γ_2^+
M	M_1^+, M_2^+
X	X_1
Z	Z_1
L	L_1^+, L_1^+
V	(V_1^+, V_1^-)
Λ	Λ_1, Λ_2
U	U_1, U_2
B	B_1, B_2

Table 9. *Kronecker products and symmetrized squares of representations for magnons*

Point	$\Gamma_i \otimes \Gamma_j$	$[\Gamma_i]^2$
M	$M_1^+ \otimes M_1^+ = \Gamma_1^+$ $M_1^+ \otimes M_2^+ = \Gamma_2^+$ $M_2^+ \otimes M_2^+ = \Gamma_1^+$	—
X	$X_1 \otimes X_1 = \Gamma_1^+ + \Gamma_2^+ + \Gamma_1^- + \Gamma_2^-$	$[X_1]^2 = \Gamma_1^+ + \Gamma_2^+ + \Gamma_1^-$
Z	$Z_1 \otimes Z_1 = \Gamma_1^+ + \Gamma_2^+ + \Gamma_1^- + \Gamma_2^-$	$[Z_1]^2 = \Gamma_1^+ + \Gamma_2^+ + \Gamma_1^-$
L	$L_1^+ \otimes L_1^+ = \Gamma_1^+ + \Gamma_2^+ + M_1^- + M_2^-$	—
V	$V_1^+ \otimes V_1^+ = \Gamma_1^+ + \Gamma_2^+ + M_1^- + M_2^-$ $V_1^+ \otimes V_1^- = \Gamma_1^- + \Gamma_2^- + M_1^+ + M_2^+$ $V_1^- \otimes V_1^- = \Gamma_1^+ + \Gamma_2^+ + M_1^- + M_2^-$	—

In evaluating $R_i \otimes R_j$ we have made use of the theory given by Bradley (4). It is an interesting feature that the Kronecker products of two representations at either L or V contain representations at points other than Γ, e.g.

$$V_1^+ \otimes V_1^+ = \Gamma_1^+ + \Gamma_2^+ + M_1^- + M_2^-. \tag{12}$$

However, this is not relevant here because the incoming photon which is absorbed to create the two magnons has momentum very nearly equal to zero, so that it belongs only to representations at Γ and not at any other special point in the Brillouin zone.

For M and L it is clear, since Γ_1^- and Γ_2^- do not occur in the Kronecker product, that the creation of two magnons at M or at L is forbidden for electric dipole radiation, but is allowed for magnetic dipole radiation. For X and Z we see that two-magnon electric and magnetic dipole absorption is possible, although the reductions

https://doi.org/10.1017/S0305004100045229 Published online by Cambridge University Press

of the symmetrized squares $[X_1]^2$ and $[Z_1]^2$ show that electric dipole absorption is only allowed for the η polarization whereas magnetic dipole absorption is allowed for all polarizations. At V we see that the creation of a pair of dissimilar magnons (V_1^+ and V_1^-) is possible by electric dipole radiation, whereas the creation of a pair of similar magnons (two V_1^+ or two V_1^-) is possible by magnetic dipole radiation. The selection rules for

Table 10. *Selection rules for two-magnon absorption*

Point	Electric dipole	Magnetic dipole
M	—	$\{M_1^+, M_1^+\}$
		$\{M_1^+, M_2^+\}$
		$\{M_2^+, M_2^+\}$
X	$\{X_1, X_1\}$	$\{X_1, X_1\}$
Z	$\{Z_1, Z_1\}$	$\{Z_1, Z_1\}$
L	—	$\{L_1^+, L_1^+\}$
V	$\{V_1^+, V_1^-\}$	$\{V_1^+, V_1^+\}$
		$\{V_1^-, V_1^-\}$

The two magnons which may be created possess the symmetries shown between the brackets.

two-magnon absorption of unpolarized radiation are summarized in Table 10. Since two-magnon electric dipole absorption is allowed at a general **k** the most significant result is probably that this process is forbidden at M and L.

We are indebted to Miss N. A. Begum, Prof. R. Loudon, Dr J. B. Parkinson and Dr J. A. Reissland for helpful discussions, and one of us (S. J. J.) is indebted to the Plessey Company for financial support.

REFERENCES

(1) Altmann, S. L. and Cracknell, A. P. Lattice harmonics I. Cubic groups. *Rev. Modern Phys.* **37** (1965), 19–32.
(2) Begum, N. A. and Reissland, J. A. Magnon energies in nickel oxide. *Phys. Lett.* **27A** (1968), 148–149; Reissland, J. A. and Begum, N. A., Magnons in antiferromagnetic NiO, MnO and αMnS. *J. Phys. C* (*Solid St. Phys.*) **2** (1969), 874–881.
(3) Bouckaert, L. P., Smoluchowski, R. and Wigner, E. Theory of Brillouin zones and symmetry properties of wave functions in crystals. *Phys. Rev.* **50** (1936), 58–67.
(4) Bradley, C. J. Space groups and selection rules. *J. Mathematical Phys.* **7** (1966), 1145–1152.
(5) Cracknell, A. P. Corepresentations of magnetic point groups. *Progr. Theoret. Phys.* **35** (1966), 196–213.
(6) Cracknell, A. P. and Wong, K. C. Double-valued corepresentations of magnetic point groups. *Austral. J. Phys.* **20** (1967), 173–188.
(7) Dimmock, J. O. and Wheeler, R. G. Symmetry properties of wave functions in magnetic crystals. *Phys. Rev.* **127** (1962), 391–404.
(8) Dimmock, J. O. and Wheeler, R. G. Irreducible representations of magnetic groups. *J. Phys. Chem. Solids* **23** (1962), 729–741.
(9) Koster, G. F. Space groups and their representations. *Solid State Physics* **5** (1957), 173–256.
(10) Loudon, R. Theory of infra-red and optical spectra of antiferromagnets. *Advances in Phys.* **17** (1968), 243–280.
(11) Nagamiya, T., Yosida, K. and Kubo, R. Antiferromagnetism. *Advances in Phys.* **4** (1955), 1–112.

https://doi.org/10.1017/S0305004100045229 Published online by Cambridge University Press

(12) ROOKSBY, H. P. A note on the structure of nickel oxide at subnormal and elevated temperatures. *Acta cryst.* **1** (1948), 226.

(13) ROTH, W. L. Magnetic structures of MnO, FeO, CoO and NiO. *Phys. Rev.* **110** (1958), 1333–1341; Multispin axis structures for antiferromagnets. *Phys. Rev.* **111** (1958), 772–781.

(14) SHUBNIKOV, A. V. and BELOV, N. V. *Colored symmetry*. (Pergamon Press; Oxford, 1964).

(15) SHULL, C. G., STRAUSER, W. A. and WOLLAN, E. O. Neutron diffraction by paramagnetic and antiferromagnetic substances. *Phys. Rev.* **83** (1951), 333–345.

(16) SLACK, G. A. Crystallography and domain walls in antiferromagnetic NiO crystals. *J. Appl. Phys.* **31** (1960), 1571–1582.

(17) SLATER, J. C. *Quantum theory of molecules and solids*, volume 2 (McGraw-Hill; New York, 1965).

(18) UCHIDA, E., FUKUOKA, N., KONDOH, H., TAKEDA, T., NAKAZUMI, Y. and NAGAMIYA, T. Magnetic anisotropy of single crystals of NiO and MnO. *J. Phys. Soc. Japan* **23** (1967), 1197–1203.

(19) YAMADA, T. Magnetic anisotropy, magnetostriction, and magnetic domain walls in NiO. I. Theory. *J. Phys. Soc. Japan* **21** (1966), 664–671.

(20) YAMADA, T., SAITO, S. and SHIMOMURA, Y. Magnetic anisotropy, magnetostriction, and magnetic domain walls in NiO. II. Experiment. *J. Phys. Soc. Japan* **21** (1966), 672–680.

https://doi.org/10.1017/S0305004100045229 Published online by Cambridge University Press